Identification and analysis of new α- and β-hydroxy ketones related to the formation of 3-methyl-2,4-nonanedione in musts and red wines.

Ana Peterson, Céline Cholet, Laurence Gény, Philippe Darriet, Yannick Landais, Alexandre Pons

HAL Id: hal-02619931
https://hal.inrae.fr/hal-02619931

Submitted on 20 Jul 2022

Identification and analysis of new α- and β-hydroxy ketones related to the formation of 3-methyl-2,4-nonanedione in musts and red wines

Ana Peterson[1,*], Céline Cholet[1], Laurence Geny[1], Philippe Darriet[1], Yannick Landais[2], Alexandre Pons[1,3]

[1]*Université de Bordeaux, Unité de recherche OEnologie, EA 4577, USC 1366 INRA, ISVV, 33882*

Villenave d'Ornon cedex, France

[2]*Université Bordeaux, ISM, CNRS UMR 5255, Talence, France*

[3]*Seguin Moreau Cooperage, ZI Merpins, 16103 Cognac, France*

*Corresponding author: Université Bordeaux, ISVV, EA 4577, Unité de recherche Oenologie, F-33882
Villenave d'Ornon, France. *Email address:* anapete@gmail.com

1   ABSTRACT

2   The formation of 3-methyl-2,4-nonanedione (MND) during red wine aging can contribute to the

3   premature evolution of aroma, characterized by the loss of fresh fruit and development of dried fruit

4   flavors. The identification of two new hydroxy ketones, 2-hydroxy-3-methylnonan-4-one (*syn-* and *anti-*

5   ketol diastereoisomers) and 3-hydroxy-3-methyl-2,4-nonanedione (HMND), prompted the investigation

6   of the precursors and pathways through which MND is produced and evolves. An HS-SPME-GC-MS

7   method was optimized for their quantitation in numerous must and wine samples, providing insight into

8   the evolution of MND, HMND, and ketols through alcoholic fermentation and wine aging. Alcoholic

9   fermentation resulted in a significant decrease in MND and HMND and the simultaneous appearance of

10   ketol diastereoisomers. The analysis of 167 dry red wines revealed significant increases in MND and *anti-*

11   ketol contents through aging and a significant positive correlation between MND and *anti*-ketols.

12   Additional experiments demonstracted that ketols are precursors to MND during red wine oxidation.

13   Keywords: wine, oxidation, premature aging, 3-methyl-2,4-nonanedione, hydroxy ketones, aroma

14   precursor

Introduction

16 The development of wine aroma through low and gradual oxygen exposure during aging is often positive

17 in red wines, but can be unfavorable in many cases, resulting in a rapid loss of fresh, fruity flavors.

18 Prematurely aged wines are marked by intense prune and fig aromatic nuances that dominate the desirable

19 bouquet achieved through aging (Picard et al., 2015). This aromatic defect, in part, is caused by the

20 presence of 3-methyl-2,4-nonanedione (MND **1**, Figure 1) in concentrations above its detection threshold

21 (A. Pons, Lavigne, Darriet, & Dubourdieu, 2013; A. Pons, Lavigne, Eric, Darriet, & Dubourdieu, 2008).

22 The production of a high level of MND in the early stages of aging is believed to negatively impact wine

23 quality and aging potential.

24 The oxygen consumption and aging potential of red wines depends significantly on their phenolic,

25 antioxidant, and transition metal contents (Danilewicz, 2003; Ferreira & Carrascon, 2015; Waterhouse &

26 Laurie, 2006). The composition of certain oxidizable substrates can also impact red wine quality over

27 time. In wine, the oxidation of higher alcohols produces odorous aldehydes, as is the case with the

28 oxidation of 3-methyl-1-butanol to 3-methylbutanal (Culleré, Cacho, & Ferreira, 2007). Thus,

29 determining the precursors of MND and methods by which they can be screened is an important step in

30 being able to predict the aging potential of red wines.

31 MND has been identified as a potent odorant in many other products, including cooked spinach (Naef &

32 Velluz, 2000), dried herbs (Sigrist, Manzardo, & Amadò, 2002), oxidized soybean oil (Guth & Grosch,

33 1990), green and black tea (Guth & Grosch, 1993), and various species of fish. It has also been measured

34 in aroma distillates of fresh apricots and organic extracts of prunes and figs (A. Pons et al., 2008). It is

35 responsible for the "hay-like off-flavor" in dry spinach (Masanetz, Guth, & Grosch, 1998) and has been

36 identified as a "light-induced off-flavor" in degraded or "reversed" soybean oil (Guth & Grosch, 1990,

37 1991; Sano et al., 2017). Investigations into the production of MND through the photooxidative

38 degradation of dried herbs/vegetables (Sigrist et al., 2002), green tea (Sigrist, 2002), and soybean oil

39 (Guth & Grosch, 1991; Sano et al., 2017), revealed that two furan fatty acids (FFA) from the dimethyl

furan family, 9-(3,4-dimethyl-5-pentyl-2-furyl)nonanoic acid (F3 acid) and 11-(3,4-dimethyl-5-pentyl-2-furyl)undecanoic acid (F6 acid) (Figure SM1), are significant precursors in these foods. The presence and oxidative degradation of these dimethyl FFA have been hypothesized in certain red wines and are currently under investigation (A. Pons, Lavigne, Darriet, & Dubourdieu, 2012). We believe, however, that there are additional pathways through which MND forms and evolves in wine that merit further investigation.

The diastereoisomers of 2-hydroxy-3-methylnonan-4-one (*anti*-ketol **3a** and *syn*-ketol **3b**, Figure 1) are β-hydroxyketones that were detected and identified after alcoholic fermentation (*S. cerevisiae*) of MND-spiked synthetic must, in conjunction with a significant decrease in MND (Allamy, Darriet, & Pons, 2018). Previous studies have shown that ketoreductases, specifically baker's yeast (*S. cerevisiae*), can reduce β-diketones to β-hydroxyketones with high diastereo- and enantiostereoselectivity and are employed as biocatalysts in the high-yielding synthesis of non-racemic chiral alcohols (Nakamura, Yamanaka, Matsuda, & Harada, 2003; Yildiz, Canta, & Yusufoglu, 2014). Based on the structure of the ketols **3a** and **3b** and their connection to MND, we hypothesized that their presence in wine could provide another pathway for the formation of MND. To investigate this preliminary finding further, it was necessary to optimize the quantitation of the ketol diastereoisomers in musts and dry red wines.

The α-hydroxy-β-diketone, 3-hydroxy-3-methyl-2,4-nonanedione (HMND **2**, Figure 1), was first discovered through studies on the photo-oxidation products of MND (Sigrist, Giuseppe, & Amado, 2003) and dimethyl FFA (Sigrist, 2002). It was identified in green tea extracts and its addition to teas improved their creamy, buttery notes and typical mouthfeel of green tea (Naef, Jaquier, Velluz, & Maurer, 2006). This property was exploited in a patent for the use of HMND as a flavoring ingredient (WO 2006/092749 A1, 2006). HMND was generated in soybean oil under photooxidative conditions and was found to contribute to the off-odor of degraded soybean oil (Sano et al., 2017). Its production in green tea and dried herbs during light exposure experiments occurred in addition to that of MND (Sigrist, 2002).

64   Considering that both dimethyl FFA and MND have been found in wine, the presence of HMND in these

65   products was likely.

66   Based on the structure of the ketols **3a** and **3b** and their connection to MND, we hypothesized that their

67   presence in wine could provide another oxidative pathway for the formation of MND. A method using

68   headspace solid phase microextraction (HS-SPME) followed by gas chromatography ion trap mass

69   spectrometry with chemical ionization (GC-MS-CI) was optimized to analyze musts and dry red wines for

70   the content of all ketones displayed in Figure 1. After establishing the presence of ketols **3a** and **3b** at

71   quantifiable levels in numerous assayed red wines, their oxidation in a young red wine was monitored to

72   evaluate their role as precursors of MND. The content of HMND was also monitored during the

73   experiment to investigate whether the oxidation of MND in wine resulted in the production of HMND.

74   **2. Materials and Methods**

75   **2.1** *Chemicals and reference compounds*

76   Ammonium sulfate ($\geq$99.9%), 3-octanol (99%), ethylenediaminetetraacetic acid (EDTA, $\geq$99%) and

77   alkanes (C_8-C_{20}, 40 mg/L in hexane), [1,2-Bis(diphenylphosphino)ethane]dichloronickel(II)

78   ([NiCl$_2$(dppe)]), acetaldehyde (anhydrous, $\geq$99.5%), ammonium chloride (NH$_4$Cl), diethylether (Et$_2$O,

79   ACS grade) were purchased from Sigma-Aldrich (Saint-Quentin Fallavier, France). Ethanol absolute

80   (>99.7%) was obtained from VWR Chemicals (Fontenay-sous-Bois, France). 3-Methyl-2,4-nonanedione

81   (99%) was purchased from Chemos GmbH (Regenstauf, Germany). Ultra-pure water was used in all

82   sample preparations and model wines (Milli-Q, Millipore, Bedford, MA, USA). 3-Hydroxy-3-methyl-2,4-

83   nonanedione (>95%) was purchased from Synnovator, Inc. (North Carolina, USA). Octen-3-ol (98%),

84   lithium triethylborohydride (LiBHEt$_3$, 1M in THF), magnesium sulfate (MgSO$_4$, anhydrous), and

85   magnesium bromide (MgBr$_2$, 98%, anhydrous) were purchased from Fisher Scientific (Illkirch, France).

86   **2.2** *Origins of musts and wines*

87　The contents of MND **1**, HMND **2**, *anti*-ketol **3a**, and *syn*-ketol **3b** were determined in musts and their

88　resulting dry red wines after alcoholic fermentation. Musts were obtained from grapes harvested at

89　different levels of maturity in September 2016 and 2017 from three commercial plots in the Gironde

90　network, "Bordeaux raisins," located in Saint-Émilion, Pauillac and Entre-Deux-Mers. After harvest, 10

91　clusters were crushed, and the juice was frozen (-20°C) until analysis. All must samples were thawed at

92　room temperature and centrifuged for five min at 10,000 G prior to analysis to remove solid material.

93　The vintage, variety, region, and number of must samples analyzed are displayed in Table SM1.

94　Additional dry red wines of varying vintages were analyzed and were donated from numerous wineries in

95　the Bordeaux region as well as from Switzerland (Ticino) and the United States (Virginia, Napa Valley).

96　**2.3** *Synthesis of ketols* **3a** *and* **3b**

97　The keto-aldol diastereomeric mixture was synthesized according to previously published procedures

98　(Cuperly, Petrignet, Crévisy, & Grée, 2006), which employed a nickel hydride catalyst. A 1M solution of

99　LiBHEt$_3$ in THF (570 μL, 0.567 mmol) was added to a solution of [NiCl$_2$(dppe)] (300 mg, 0.567 mmol)

100　in anhydrous THF (30 mL) at room temperature under argon. After stirring for 5 min, the reaction

101　mixture was transferred to a flask (under argon) containing MgBr$_2$ (100 mg, 0.567 mmol) and stirred for

102　an additional 5 min, then cooled to -50°C. Acetaldehyde (1.2 mL, 20.8 mmol) and octen-3-ol (1.8 mL,

103　18.9 mmol) were added, after which the temperature was raised to room temperature. The reaction was

104　monitored by thin layer chromatography (TLC) until the disappearance of octen-3-ol. The reaction

105　mixture was quenched with a saturated solution of NH$_4$Cl (75 mL). The aqueous phase was extracted with

106　Et$_2$O (3 x 150 mL). The organic phase was dried (MgSO$_4$) and concentrated under vacuum. Purification

107　performed by column chromatography on silica gel (pentane/Et$_2$O, 4.55:1 then 2:1 v/v) afforded an

108　inseparable mixture of diastereoisomeric aldols (**3a** and **3b**) as a pale, yellow oil (Figure SM2). The purity

109　of the *anti/syn*-ketol mixture was 97% as determined by gas chromatography with flame ionization

110　detection (GC-FID). The percent of each diastereomer present in the synthesized standard was calculated

111　by integration of the carbinol proton (C*H*OH) signals at 4.09 and 3.90 ppm. According to the literature

112 regarding the assignment of the relative configurations of α-alkyl-β-hydroxy ketone stereoisomers, the

113 *syn*-stereoisomer signal is observed further downfield (4.09 ppm) than that of the *anti*-stereoisomer (3.90

114 ppm) (Kalaitzakis & Smonou, 2008). The synthesis was found to yield the diastereoisomers in a 68.5:31.5

115 *syn/anti* ratio.

116 *Nuclear Magnetic Resonance Spectroscopy (NMR):* [1]H spectra were recorded on a Bruker Avance I ([1]H:

117 300 MHz), spectra referenced using the lock frequency of deuterated solvent. Chemical shifts (δ) and

118 coupling constants (J) are expressed in ppm and Hz, respectively. Thin-layer chromatography (TLC) was

119 performed on 60F TLC plates: thickness 0.25mm, particle size 10 µm, pore size 60 Å. Merck silica gel 60

120 (70–230 mesh and 0.063–0.200 mm) was used for column chromatography.

121 (*syn, anti*) ^{1}H NMR (300 MHz, Chloroform-*d*): δ 4.09 (*syn*) (qd, J = 6.4, 3.3 Hz, 1H, C*H*OH), 3.90 (*anti*)

122 (p, J = 6.5 Hz, 1H, C*H*OH), 2.62 – 2.36 (*syn/anti*) (m, 3H, C*H*(CH$_3$)CO and C*H*$_2$CO), 1.64 – 1.49 (m, 2H,

123 COCH$_2$C*H*$_2$), 1.38 – 1.21 (m, 4H, CH$_2$C*H*$_2$CH$_2$ and CH$_2$C*H*$_2$CH$_3$), 1.19 (*anti*)(d, J = 6.3 Hz, 3H,

124 C*H*$_3$CHOH), 1.15 (*syn*)(d, J = 2.0 Hz, 3H, C*H*$_3$CHOH), 1.12 (*syn*)(d, J = 2.8 Hz, 3H, CH(C*H*3)CHOH),

125 1.10 (*anti*)(d, J = 7.2 Hz, 3H, CH(C*H*3)CHOH), 0.93 – 0.84 (*syn/anti*) (t, 3H, CH$_2$C*H*$_3$).

126 **2.4** *Quantitation of MND* **1**, *HMND* **2**, *anti-ketol* **3a**, *and syn-ketol* **3b** *in must and wine*

127 **2.4.1** *Sample preparation and HS-SPME extraction*

128 The sample preparation method was adapted from a previously published assay technique (Allamy et al.,

129 2018). Ultra-pure water (9 mL) and the sample (1 mL) were placed in a 20 mL amber SPME vial

130 containing 5 g ammonium sulfate, 5 µL EDTA solution (60 g/L, H$_2$O), and 10 µL of the internal standard

131 (IS, 5 mg/L 3-octanol, EtOH). The oxygen in the headspace of the vial was purged with carbon dioxide

132 and the vial was sealed with a PTFE-lined cap. A 65 µm polydimethylsiloxane-divinylbenzene

133 (PDMS/DVB, Supelco, Lyon, France) fiber was used for headspace solid phase microextraction (HS-

134 SPME) of samples. Using the Combi PAL autosampler (CTC Analytics, Zwingen, Switzerland), samples

135 were incubated at 50°C for 7 min prior to fiber extraction, followed by extraction for 20 min at an

136 agitation speed of 460 rpm.

2.4.2 *Gas Chromatography-Mass Spectrometry Conditions*

138 The fiber was desorbed into the injection port (Varian 1177, 250°C) of a CP3800 Gas Chromatograph

139 (Varian/Agilent) for 9 min. The injector was set to splitless mode initially (closure time: 1 min) after

140 which a split flow of 50 mL/min was used. Separation was performed on a BP20 column (60 m x 0.25

141 mm, 0.5 μm film thickness, SGE), which was coupled to a Varian/Agilent Technologies 4000 ion trap

142 mass spectrometer. The carrier gas was helium (Air Liquide, Bordeaux) with a flow rate of 1.5 mL/min.

143 The oven temperature program was adapted from previous work (Allamy et al., 2018) to achieve good

144 chromatographic separation in a shorter amount of time. The oven temperature was set to 45°C (1 min

145 hold) and increased to 210°C at 7°C/min followed by a ramp of 100°C/min to 250°C (6 min hold). The

146 transfer line, trap, and manifold were maintained at 230°C, 150°C and 50°C, respectively. All compounds

147 were ionized using internal positive chemical ionization (CI) with methanol as reactant gas. The 31-min

148 acquisition period was divided into the four segments: IS (15-17 min, *m/z* 68-120), HMND **2** (20-21.8

149 min, MS/MS, precursor ion *m/z* 169), MND **1** (21.8-23 min, μSIS, *m/z* 171), and *anti-* and *syn-*ketols **3a**

150 and **3b** (23-26 min, MS/MS, precursor ion *m/z* 173). These parameters are described in further detail in

151 Table SM2.

152 Linear retention indices (LRI) were determined for all tested compounds on the same Varian/Agilent

153 system described above (van Den Dool & Dec. Kratz, 1963). Pure standards of all tested compounds and

154 a series of alkanes (C_8-C_{20}, 40 mg/L in hexane) were injected on the 1177 injector in splitless mode

155 (230°C, purge time: 1 min, purge flow: 50 mL/min) on a polar BP20 capillary column (SGE, France, 50

156 m x 0.22 mm, 0.25 μm film thickness) and a non-polar BPX5 column (SGE, 50 m x 0.22 mm, 0.25 μm

157 film thickness). The GC oven temperature was initially set at 45°C for 1 min, then raised to 240°C at

158 3°C/min and finally held at that temperature for 20 min. The carrier gas was He with a flow rate of 1

159 mL/min. Data were collected in EI full scan mode (*m/z* 40-250) with an emission current at 10 μA and

160 electron energy of 70 eV.

161 **2.4.3** *MS/MS Ionization Parameters Optimization*

162 Mass spectrometric parameters for MND **1** were optimized previously (A. Pons, Lavigne, Darriet, &

163 Dubourdieu, 2011). Given the similar structures of HMND **2** and ketols **3a** and **3b** to **1**, it was

164 hypothesized that chemical ionization would be best suited for their analysis by MS. Mass spectra were

165 recorded for pure standards of **2** and **3a/b** in full scan mode by CI and electron impact (EI), providing

166 information on the molecular and precursor ions for each structure. Model wine solutions containing 10

167 µg/L of each compound (separately) were extracted by the SPME method and analyzed in full scan mode

168 (*m/*z 45-250) by both types of ionization.

169 Optimization of the resonant excitation conditions for MS/MS analysis was performed with Automated

170 Methods Development (AMD) methods. Experiments were conducted step by step at a constant stability

171 parameter/excitation storage ($q = 0.2$-0.4) and 6 excitation amplitude values (0.2-1.2V). An optimized

172 excitation amplitude was chosen based on comparison of the compound signal abundances for each value.

173 The excitation storage level was chosen by comparing the most abundant signals obtained for each q

174 value. Table SM1 displays the optimized parameters for each acquisition segment. The ion *m/*z 99 was

175 extracted as the quantitative ion for **2**, **3a**, and **3b** as it was the most abundant ion in the CI MS spectra

176 (after the precursor ion) of these structures.

177 **2.4.4** *Quantitation in must and wine*

178 The concentrations of all analytes were determined by the standard addition method. Stock solutions were

179 prepared separately for each compound from pure standards and subsequently added to a dry red wine at

180 increasing concentrations to cover the approximate range found in wine: 40-240 ng/L for MND **1**, 25-200

181 ng/L for HMND **2**, 150-2250 ng/L for *anti*-ketol **3a**, and 250-4000 ng/L for *syn*-ketol **3b**. Calibration was

182 performed in different red wines for each compound, which were chosen for their relatively low levels of

183 analytes. For quantitation of all compounds in must, calibration curves were also constructed in different

184 must samples in the following concentration ranges: 40-280 ng/L for **1**, 25-300 ng/L for **2**, 60-750 ng/L

185 for **3a**, and 140-1640 ng/L for **3b**. The concentrations of **3a** and **3b** added to wines and musts were

186 determined according to the ratio between the two diastereoisomers given by ^{1}H NMR analysis of the

187 synthesized standard (Section 2.3). All spiked wines and musts were analyzed in duplicate to construct

188 calibration curves. Analyte peak areas were obtained by integration of their extracted quantitative ions:

189 *m/z* 171 (**1**) and *m/z* 99 (**2**, **3a**, **3b**) and compared against that of the internal standard, 3-octanol (*m/z* 71).

190 **2.5** *Method Evaluation and Validation*

191 Limits of detection (LOD) and quantitation (LOQ) were determined by three and ten times the standard

192 deviation between seven replicate extractions of different wine/must samples, each containing relatively

193 low concentrations of the analytes. The method linearity was evaluated by the regression coefficient R^2 for

194 each standard addition curve in must and red wine. The minimum concentration for the linear range of an

195 analyte was established by its LOQ. Precision was evaluated by the percent residual standard deviation

196 determined from the seven replicate extractions. The accuracy of the method was determined by the

197 analysis of a red wine and must (distinct from the samples used for calibration, detection limits, and

198 linearity evaluation) unspiked and spiked with MND **1** (100 ng/L), HMND **2** (100 ng/L), *anti*-ketol **3a**

199 (126 ng/L) and *syn*-ketol **3b** (274 ng/L). The percent spike recovery (%R) was calculated for each

200 compound using %R = $(C_{sp}-C_{usp})/C_{spa}$, where C_{sp} is the concentration of the analyte in the spiked

201 wine/must, C_{usp} is the concentration of the analyte in the unspiked wine/must, and C_{spa} is the

202 concentration of the spike added. The effect of pH on the relative responses of each analyte was evaluated

203 in a dry red wine adjusted to pH 3.5 and 4.0. The impact of ethanol concentration on analyte responses

204 was also evaluated by the analysis of a dry red wine (pH 3.5) adjusted to 12% and 15% ethanol. The

205 relative responses (with respect to the internal standard) were calculated and compared between pH levels

206 and ethanol concentrations.

207 **2.6** *Determining the Detection Threshold of HMND* **2** *and Ketols* **3a/3b** *in Model Wine*

208 All detection thresholds were determined according to the 3-alternative forced choice procedure (3-

209 AFC)(AFNOR, 2007) in model wine solution (12% double-distilled ethanol, 5 g/L tartaric acid, pH 3.5).

210 The pH of the solution was adjusted with NaOH pellets. Three sessions were performed for each

211 compound to define the appropriate concentration range for detection and to confirm the threshold level.

212 The solutions were presented in AFNOR (Association Française des Normes) standard glasses in

213 ascending order with respect to odorant concentration. Reference standards of the odorants were dissolved

214 in ethanol (20 g/L) followed by stepwise dilution with ethanol and addition to the model wine solution.

215 For each of the six concentrations, subjects received a set of three glasses labeled with three-digit random

216 codes. Two of these glasses contained model wine (blank samples) while one contained the odorant at

217 increasing concentrations. The odor detection threshold was defined at which the probability of detection

218 was 50% (AFNOR, 2007). The sensory panel consisted of 18 experienced assessors present at the day of

219 the analysis: students and researchers (4 male, 14 female) between 20 and 40 years old with research

220 experience in the assessment of wine flavors.

221 **2.7** *Experiments to study the effects of ketol additions on the MND content of red wine*

222 To a young (2017), newly bottled dry red wine, the ketol standard (synthesized in this work) was added to

223 obtain two different total ketol concentrations (10 µg/L and 20 µg/L). Spiked and control (no ketol

224 addition) wines (30 mL) were placed in 45 mL capped glass flasks, providing headspace and thus oxygen

225 to all samples. Three replicates of each 'treatment' were prepared in this way and were analyzed several

226 times over the course of 35 days. Small additions of oxygen were introduced into samples each time

227 flasks were opened for analysis.

228 **2.8** *Statistical Analysis*

229 The homogeneity of variance (Levene's test) and normality of residuals (Shapiro-Wilk test) were verified

230 before application of one- and two-way ANOVA. Differences and correlations between data sets that did

231 not satisfy the normality assumption were evaluated by Kruskal-Wallis nonparametric test and Spearman

232 rank-order correlation test. Paired data sets that were found to have non-normal distributions were

233 analyzed by the Wilcoxon signed rank test for paired samples. All statistical tests were performed using R

234 software (R foundation for Statistical Computing, England).

235 **3. Results and Discussion**

236 **3.1** *Method Optimization and Validation*

237 **3.1.1** *Mass Spectrometric Optimization*

238 The mass spectrometric parameters for HMND **2** and ketols **3a/3b** were optimized through AMD

239 methods. Fragmentation and selective ion storage (MS) alone did not provide sufficient selectivity or

240 sensitivity for the detection of **2** and **3a/3b** so MS/MS was optimized and employed for these analytes.

241 The excitation storage levels and amplitudes that yielded the highest signal-to-noise ratio for **2** and **3a/3b**

242 were selected (Table SM2). Precursor ions to test for each compound were chosen based on the relative

243 abundances in mass spectra obtained in full scan mode (Figure SM3 and SM4). The ionization of **2** by EI

244 provided no signal under these conditions so optimization proceeded using CI. Optimization for **3a** and

245 **3b** proceeded with testing CI and EI, as both provided signals. For **3a/3b**, *m/z* 173 (M+H ion) and *m/z* 117

246 were tested for MS/MS in CI and EI mode, respectively. Two ions were tested in CI mode for **2**: *m/z* 187

247 (M+H ion) and *m/z* 169. After optimization of the excitation storage level and amplitude for each

248 precursor ion, analysis of real wine samples supplemented with **2** revealed that using *m/z* 169 as a

249 precursor ion produced a detectable signal. The mass spectrum of **2** in EI mode is also displayed in Figure

250 SM3 (B) as a confirmation of the compound's fragmentation pattern as reported previously (Sigrist et al.,

251 2003).

252 The chromatographic conditions provided good separation of all compounds, including the two ketol

253 diastereoisomers, **3a** and **3b** (Figure SM5). Resolution between the ketol diastereoisomer peaks was

254 sufficient (R=1.13) for individual integration and quantitation of ketol responses. Hydroxy ketones **2**, **3a**,

255 and **3b** were identified in red wine and must based on GC-MS by comparing their mass spectra and LRI

256 with those of synthesized pure compounds (Table SM3). Pure compounds were also co-injected with

257 wine and must samples, enabling their identification for the first time in must and wine. The LRI values

258 for **1** differed from those previously reported (Allamy et al., 2018; A. Pons et al., 2008) as the system

259 used and laboratory in which LRI values were obtained were different. The literature reports LRI values

260 for **1** ranging from 1703 (Triqui & Bouchriti, 2003) to 1762 (Stephan & Steinhart, 1999) on polar

261 columns and between 1242 (Schuh & Schieberle, 2006) and 1253 (Milo & Grosch, 1993) on non-polar

262 columns.

263 **3.1.2** *Effect of pH and ethanol content*

264 Because the ethanol concentration and pH level of a matrix has been shown to influence the equilibrium

265 and extraction efficiency of certain volatile compounds (Câmara, Arminda Alves, & Marques, 2006),

266 these factors were evaluated for all tested compounds in dry red wines. The effect of pH on the extraction

267 yield by SPME was evaluated in red wine at pH 3.5 and 4.0. One-way ANOVA analysis of the resulting

268 relative response means gave p values greater than 0.05 (p_1=0.723; p_2=0.897; p_{3a}=0.560; p_{3b}=0.663),

269 revealing that there were no significant differences between extraction yields with tested pH levels (Table

270 SM4). The influence of ethanol concentration on the extraction yield was also evaluated in red wine at 12

271 and 15% ethanol. One-way ANOVA analysis of the relative response means gave p values greater than

272 0.05 (p_1=0.902; p_2=0.616; p_{3a}=0.957; p_{3b}=0.417), indicating that there were no significant differences

273 between analyte extraction yields with tested ethanol contents (Table SM4).

274 **3.1.2** *Method linearity, detection limits, and precision*

275 Having optimized the extraction and GC-MS parameters of the method, the linearity, detection limits, and

276 precision were evaluated in dry red wine and must. The method showed acceptable linearity ($R^2 > 0.990$) in

277 wine for all assessed compounds in the ranges displayed in Table 1. Calibration curves for HMND **2**, *anti-*

278 ketol **3a**, and *syn*-ketol **3b** had slope values of the same order of magnitude, while that of MND **1** was an

279 order of magnitude greater. The method was most sensitive for **1** and **2**, evidenced by their LOD values for

280 **3a** and **3b**. It appears that the sensitivity of the method is significantly decreased by the lack of a second

281 carbonyl group (and replacement by a hydroxyl group) in the ketone structure. Overall, the method

282 provided sufficient sensitivity for the analysis of all analytes in must and wine. All LOD values for

283 assessed compounds were below 50 ng/L in both red wine and must, enabling their detection in most

284 assayed samples. Determination of the percent recovery of each analyte spiked into a red wine was used to

285 evaluate the accuracy of the method and is expressed as the Recovery % in Table 1. Percent recovery

286 values were between 93 and 99%, indicating high accuracy for the quantitation of all four analytes in red

287 wine.

288 The method performance was also evaluated in musts to enable the analysis of analytes before and after

289 alcoholic fermentation. The linearity in must was satisfactory ($R^2 > 0.990$) in the ranges specified in Table

290 1. The analytical method was most sensitive for **1** in must, which is indicated by an LOD value more than

291 5 times lower than those of **2**, **3a**, and **3b**. Detection limits in must were comparable to those calculated in

292 wine for all compounds except for **2**, which had an LOD in must that was four times the value calculated

293 in wine. However, this level was still sufficient to quantitate **2** in the majority of assayed must samples.

294 It has been shown that an increase in ethanol content generally decreases the extraction yield of volatile

295 compounds by SPME (Câmara et al., 2006; Correia, Delerue-matos, & Alves, 2000). While this effect

296 was observed for compounds **1** and **3b** through comparing LOD values in wine and must, the opposite

297 trend was observed for compounds **2** and **3a**. Although must contains no ethanol and would be expected

298 to provide higher analyte extraction and thus higher LOD values, the high sugar content (>200 g/L) is an

299 interference that can also affect SPME efficiency. For this reason, calibration was performed separately in

300 must for analyte quantitation in this matrix. The quantitation of all analytes in must was found to be

301 reasonably accurate as evidenced by percent recovery values between 93 and 95% (Table 1).

302 **3.2** *Application of method to musts and young red wines: Effects of alcoholic fermentation*

303 To improve our understanding of the changes the analytes undergo during alcoholic fermentation, the

304 optimized HS-SPME-GC/MS method was used to quantitate analytes in must samples and in the resulting

305 wine just after alcoholic fermentation. The concentration means of all assayed compounds were

14

306 significantly different between must and wine samples (Wilcoxon, *p* <0.0001). Further evidence for the

307 hypothesized reduction of MND **1** to *syn-* and *anti-*ketols **3a** and **3b** was obtained from the analysis of red

308 wine must samples and their resulting wines. The content of **1** was found to be significantly lower in

309 wines just after alcoholic fermentation (Figure 2, **A**). Must samples contained trace amounts of **3a** and **3b**.

310 After fermentation, however, all analyzed samples contained detectable levels of both diastereoisomers

311 (Figure 2, **C** and **D**). The average concentration of *anti*-ketol **3a** (37.0 ng/L) in these young wines was

312 below its limit of quantitation while that of *syn*-ketol **3b** just after alcoholic fermentation (158.8 ng/L)

313 was significantly higher than that of **3a** (Wilcoxon, *p*=2.2e-16) and accounted for an average of 81% of

314 the total ketol content. Previous studies support this finding as they have shown that the reduction of 3-

315 methyl-2,4-diketones with Baker's yeast (BY) resulted in a mixture of both *syn-* and *anti*-ketol products,

316 with the *syn* stereoisomer accounting for 80% of the mixture (Fauve & Veschambre, 1988). The chemical

317 synthesis of the ketols performed in this study also favored the formation of the *syn* isomer (68.5%).

318 The production of HMND by the photo-oxidation of MND has been previously reported (Sigrist et al.,

319 2003). The photo-oxidation of MND in grapes during ripening provides a possible explanation for higher

320 levels of this hydroxy ketone in musts. The significant decrease in HMND **2** after alcoholic fermentation

321 (Figure 2, **B**) accounts for the low levels found in bottled dry red wines (see Section 3.3). The reduction

322 of this diketone by *S. cerevisiae* may yield other hydroxyketones that have yet to be identified in wine.

323 **3.3** *Application of method to dry red wines: Evolution during bottle aging*

324 The evolution of the tested compounds during aging was investigated by the analysis of numerous (167)

325 dry red wines from various regions and vintages (Table SM5). It is clear from these results that bottle

326 aging plays a critical role in the evolution of MND **1** and the *anti*-ketol **3a**. Contrary to the wine samples

327 analyzed just after fermentation (Figure 2, Section 3.2), MND concentrations exceeded 300 ng/L in a few

328 aged wines and both ketol maximum concentrations exceeded 1000 ng/L. HMND levels were below 70

329 ng/L in all assayed dry red wines and in many cases, HMND was not detected at all. The set of 167 red

330 wines was divided into two groups by bottle aging time: wines aged for less than 6 years and those aged

15

331   for 6 years or more. The average concentrations of each analyte for these two groups are displayed in

332   Table 2. While the average concentrations of MND **1** and *anti*-ketol **3a** increased by 2.4 and 1.5 times,

333   respectively, the average concentrations of HMND **2** and *syn*-ketol **3b** did not change significantly with

334   aging time. The HMND content did not vary greatly between regions or aging time and appears to

335   continue to degrade after fermentation as its content in aged dry red wines was low compared to wines

336   just after fermentation. The differences between the ketol contents of wines just after fermentation and

337   after a year or more of aging indicate that an additional formation pathway must exist in dry red wines.

338   The ratio between **3a** and **3b** further indicates the continuous evolution of **3a** through aging, ultimately

339   becoming the dominant ketol diastereoisomer.

340   Table 3 displays the analysis of a selection of wines from the 167 that were tested. Two wines, separated

341   by 6 to 10 years of aging time, were selected from the same chateau in various regions. Although we

342   cannot make any assumptions about the effect of climate and region on the analytes with such a small

343   subset of data, this provides a glimpse of the concentration ranges we observed in the large set of wines

344   analyzed in this study. In all wines excepting those from Virginia, the MND content and *anti:syn*-ketol

345   ratio appeared to correlate positively with age. Additionally, a higher ketol ratio provided a higher MND

346   content. This was particularly evident in the wines from Napa, which accounted for the highest MND and

347   *anti*-ketol contents determined in the 167 assayed wines.

348   As it has already been shown that MND increases with oxygen exposure (A. Pons et al., 2013), the next

349   line of inquiry was whether any link could be found between the content of ketols **3a** and **3b** and that of

350   MND in the red wine data obtained. Correlation tests between the contents of each ketol diastereoisomer

351   separately, MND, and aging time (provided by the wine vintage) were performed on the results of the

352   analysis of 167 wines ranging in age from 0.5 to 28 years old (significant correlations displayed in Table

353   SM6). The Spearman rank order correlation test indicated that there was a significant positive association

354   between MND and *anti*-ketol **3a** (rho (167) =0.558, p < 0.001) and to an even greater extent between

355   MND and the *anti*: *syn*-ketol ratio (rho (167) =0.648, p < 0.001). A linear least squares regression of the

356 *anti*: *syn*-ketol ratio versus MND content displays this significant, positive correlation between the two

357 variables (R^2= 0.4574, p < 0.0001, Figure SM6). Correlation tests also provided a statistically significant

358 rho values between aging time and MND (rho (167) =0.654, p < 0.001), *anti*-ketol **3a** was positive (rho

359 (167) = 0.345, p < 0.0001) and the *anti*:*syn*-ketol ratio (rho (167)=0.499, p < 0.001).

360 **3.4** *Study of syn- and anti-ketols* **3a** *and* **3b** *as precursors of MND* **1** *in red wine*

361 In view of the statistical link between MND **1** and ketol **3a**, preliminary experiments were performed in

362 red wines to study the effect of ketols **3a** and **3b** on the formation of **1** under oxidative conditions. In

363 addition to the control samples which only contained ketols originally present, two sets of 'treated'

364 samples were monitored following the addition of 10 and 20 µg/L total ketols and storage in the presence

365 of oxygen. The high concentrations of ketols (compared to the typical range found in wine) were utilized

366 to accelerate the time in which MND formation would take place. In wines containing typical

367 concentrations of ketols (Table 1), the oxidation of ketols to MND most likely takes place over a period

368 of years. Placement of all samples in closed flasks with headspace ensured the presence of oxygen during

369 the experiment. Three replicates of each wine type (control, 10 µg/L ketols added, and 20 µg/L ketols

370 added) were prepared in this way and extracted after 10, 20, and 35 days. Only the MND concentrations

371 are shown in Figure 3 as the high ketol levels showed no significant changes during this time (the

372 increases in MND levels were small compared to ketol spiked concentrations).

373 The MND content increased by 50 ng/L and more than 100 ng/L after 35 days in samples spiked with 10

374 and 20 µg/L ketols, respectively. HMND was also monitored, but no significant changes in its content

375 were detected over the course of the experiment. A two-way ANOVA, where factor 1 was the ketol

376 addition level and factor 2 was time (days), was performed on the MND concentration data obtained

377 throughout the experiment (Table SM7). The main effects of time (F=270, p < 0.0001) as well as ketol

378 additions (F=318, p < 0.0001) on the MND concentration were found to be significant. The interaction

379 between the two factors was also significant (F=78.4, p < 0.0001), thus the MND concentrations differed

380 as a function of both time and ketol addition. This preliminary experiment has confirmed that the addition

381 of the ketol mixture to wine in the presence of oxygen can result in significant increases in the MND

382 content of the wine. We hypothesize, however, that other wine components (in addition to oxygen) are

383 involved in the conversion of these ketols to MND. We can consider ketols **3a** and **3b** to be precursors of

384 MND in red wine, but it is clear from the very slow kinetics of the conversion that this occurs over long

385 periods of aging and other hypothesized precursors likely contribute to MND formation.

386 **3.5** *Odor detection thresholds of HMND* **2** *and Ketols* **3a** *and* **3b**

387 The detection threshold of MND **1** has been well established in the context of dry wine model solutions

388 (16 ng/L) and red wine (62 ng/L) (A. Pons et al., 2013). The extremely low detection threshold allows for

389 a significant contribution to the dried fruit flavors in red wines (M. Pons et al., 2011). Detection

390 thresholds for the newly identified hydroxy ketones HMND **2** and ketols **3a** and **3b**, however, have not

391 been previously determined in model wine solution. The effect of the reduction of a carbonyl group on

392 detection thresholds has previously been shown with the 1000-fold difference between the thresholds of

393 octen-3-one (7 ng/L) and octen-3-ol (7 µg/L) (Darriet et al., 2002). A similar result was obtained for the

394 detection thresholds for the hydroxy ketones compared to that of MND. The detection thresholds of

395 racemic mixtures of **2** and **3a/3b** were determined to be 281 and 196 µg/L, respectively. It will be

396 necessary to first separate the ketol diastereoisomers before evaluating the sensory contributions of the

397 individual compounds. Taking into consideration the concentrations observed for **2**, **3a**, and **3b** in red

398 wines (Table 2 and Table 3), these hydroxy ketones do not play a significant, direct role in red wine

399 aroma.

400 **Conclusion**

401 This work presented the first identification of the *syn-* and *anti-*ketol diastereoisomers in red wines and

402 their role as precursors of MND. HMND, another ketone linked with MND, was also reported for the first

403 time in must and wine. These new hydroxy ketones were simultaneously quantitated by HS-SPME-GC-

404   MS/MS (CI, MeOH) in numerous musts and red wines (of various ages), shedding light on their behavior

405   through alcoholic fermentation and aging. The appearance of *anti-* and *syn*-ketols in young wines (18.8-

406   71.3 and 98.3-215.0 ng/L, respectively) just after alcoholic fermentation was observed concurrently with

407   the significant decrease in HMND and MND contents. *Anti*-ketols were found to correlate significantly

408   with aging time and MND content in assayed red wines ranging from 1 to 28 years old. A targeted

409   oxidation experiment of *syn-* and *anti*-ketols in red wine provided data to support the hypothesis that one

410   or both ketols are precursors to MND. Additional investigations into the precursors and pathways which

411   generate ketols during bottle aging will be performed in the future.

412   **Acknowledgements**

415   **References**

416   AFNOR. (2007). Sensory analysis-Methodology-General guidance for measuring odour, flavour and taste

417   detection thresholds by a three-alternative forced-choice (3-AFC) procedure-ISO 13301. In *Analyse*

418   *Sensorielle (7éme ed.)* (pp. 439–472).

419   Allamy, L., Darriet, P., & Pons, A. (2018). Molecular interpretation of dried-fruit aromas in Merlot and

420   Cabernet Sauvignon musts and young wines : Impact of over-ripening. *Food Chemistry*, *266*, 245–

421   253.

422   Câmara, J. S., Arminda Alves, M., & Marques, J. C. (2006). Development of headspace solid-phase

423   microextraction-gas chromatography-mass spectrometry methodology for analysis of terpenoids in

424   Madeira wines. *Analytica Chimica Acta*, *555*(2), 191–200.

425   Correia, M., Delerue-matos, C., & Alves, A. (2000). Multi-residue methodology for pesticide screening in

426   wines. *Journal of Chromatography A*, *889*, 59–67.

427   Culleré, L., Cacho, J., & Ferreira, V. (2007). An assessment of the role played by some oxidation-related

428   aldehydes in wine aroma. *Journal of Agricultural and Food Chemistry*, *55*(3), 876–881.

429   Cuperly, D., Petrignet, J., Crévisy, C., & Grée, R. (2006). From Allylic Alcohols to Aldols through a New

430   Nickel-Mediated Tandem Reaction : Synthetic and Mechanistic Studies. *Chemistry-A European*

431   *Journal*, *12*, 3261–3274.

432   Danilewicz, J. C. (2003). Review of Reaction Mechanisms of Oxygen and Proposed Intermediate

433   Reduction Products in Wine : Central Role of Iron and Copper. *American Journal of Enology and*

434   *Viticulture*, *2*, 73–85.

435   Darriet, P., Pons, M., Henry, R., Dumont, O., Findeling, V., Cartolaro, P., … Dubourdieu, D. (2002).

436   Impact Odorants Contributing to the Fungus Type Aroma from grape berries contaminated by

437   powdery mildew (Uncinula necator); Incidence of Enzymatic Activities of the Yeast Saccharomyces

438   cerevisiae. *Journal of Agricultural and Food Chemistry*, *50*, 3277–3282.

439   Fauve, A., & Veschambre, H. (1988). Microbiological reduction of acyclic β-diketones. *Journal of*

440   *Organic Chemistry*, *53*(22), 5215–5219.

441   Ferreira, V., & Carrascon, V. (2015). Oxygen Consumption by Red Wines. Part I: Consumption Rates,

442   Relationship with Chemical Composition, and Role of SO2. *Journal of Agricultural and Food*

443   *Chemistry*, *63*, 10928–10937.

444   Guth, H., & Grosch, W. (1990). Deterioration of soya-bean oil: Quantification of primary flavour

445   compounds using a stable isotope dilution assay. *Lebensmittel-Wissenschaft Und-Technologie*, *23*,

446   513–522.

447   Guth, H., & Grosch, W. (1991). Detection of Furanoid Fatty acids in Soya-Bean Oil-Cause for the Light-

448   Induced Off-Flavour. *Fat Sci. Technol.*, *93*(7), 249–255.

449   Guth, H., & Grosch, W. (1993). Identification of potent odourants in static headspace samples of green

450   and black tea powders on the basis of aroma extract dilution analysis (AEDA). *Flavour and*

451   *Fragrance Journal*, *8*(4), 173–178.

452   Kalaitzakis, D., & Smonou, I. (2008). A Convenient Method for the Assignment of Relative

453   Configuration of Acyclic α-Alkyl- β-hydroxy Carbonyl Compounds by 1H NMR. *Journal of*

454   *Organic Chemistry*, *73*, 3919–3921.

455   Masanetz, C., Guth, H., & Grosch, W. (1998). Fishy and hay-like off-flavours of dry spinach. *Zeitschrift*

456   *Fuer Lebensmittel -Untersuchung Und -Forschung A*, *206*(2), 108–113.

457   Milo, C., & Grosch, W. (1993). Changes in the Odorants of Boiled Trout (Salmo fario) As Affected by

458   the Storage of the Raw Material. *Journal of Agricultural and Food Chemistry*, *30*, 2076–2081.

459   Naef, R., & Jaquier, A. (2006). *WO 2006/092749 A1*. CH: World Intellectual Property Organization.

460   Naef, R., Jaquier, A., Velluz, A., & Maurer, B. (2006). New constituents related to 3-methyl-2,4-

461   nonanedione identified in green tea. *Journal of Agricultural and Food Chemistry*, *54*(24), 9201–

462   9205.

463   Naef, R., & Velluz, A. (2000). The volatile constituents of extracts of cooked spinach leaves (Spinacia

464   oleracea L.). *Flavour and Fragrance Journal*, *15*(5), 329–334.

465   Nakamura, K, Yamanaka, R., Matsuda, T., & Harada, T. (2003). Recent developments in asymmetric

466   reduction of ketones with biocatalysts. *Tetrahedron: Asymmetry*, *14*(18), 2659–2681.

467   Picard, M., Thibon, C., Redon, P., Darriet, P., De Revel, G., & Marchand, S. (2015). Involvement of

468   Dimethyl Sulfide and Several Polyfunctional Thiols in the Aromatic Expression of the Aging

469   Bouquet of Red Bordeaux Wines. *Journal of Agricultural and Food Chemistry*, *63*(40), 8879–8889.

470   Pons, A., Lavigne, V., Darriet, P., & Dubourdieu, D. (2011). Determination of 3-methyl-2 , 4-

471   nonanedione in red wines using methanol chemical ionization ion trap mass spectrometry. *Journal*

472   *of Chromatography A*, *1218*(39), 7023–7030.

473   Pons, A., Lavigne, V., Darriet, P., & Dubourdieu, D. (2012). Origins of 3-methyl-2,4-nonanedione in red

474   wines. In *13th Weurman Symposium*. Zaragoza, Spain.

475   Pons, A., Lavigne, V., Darriet, P., & Dubourdieu, D. (2013). Role of 3 - Methyl-2,4-nonanedione in the

476   Flavor of Aged Red Wines. *Journal of Agricultural and Food Chemistry*, *61*, 7373–7380.

477   Pons, A., Lavigne, V., Eric, F., Darriet, P., & Dubourdieu, D. (2008). Identification of volatile

478   compounds responsible for prune aroma in prematurely aged red wines. *Journal of Agricultural and*

479   *Food Chemistry*, *56*(13), 5285–5290.

480   Pons, M., Dauphin, B., La Guerche, S., Pons, A., Lavigne-Cruege, V., Shinkaruk, S., … Darriet, P.

481   (2011). Identification of impact odorants contributing to fresh mushroom off-flavor in wines:

482   Incidence of their reactivity with nitrogen compounds on the decrease of the olfactory defect.

483   *Journal of Agricultural and Food Chemistry*, *59*(7), 3264–3272.

484   Sano, T., Okabe, R., Iwahashi, M., Imagi, J., Sato, T., Yamashita, T., … Bamba, T. (2017). Effect of

485   Furan Fatty Acids and 3-Methyl-2,4-nonanedione on Light-Induced Off-Odor in Soybean Oil.

486   *Journal of Agricultural and Food Chemistry*, *65*(10), 2136–2140.

487   Schuh, C., & Schieberle, P. (2006). Characterization of the Key Aroma Compounds in the Beverage

488   Prepared from Darjeeling Black Tea : Quantitative Differences between Tea Leaves and Infusion.

489   *Journal of Agricultural and Food Chemistry*, *2*, 916–924.

490   Sigrist, I. A. (2002). *Investigation on aroma active photooxidative degradation products originating from*

491   *dimethyl pentyl furan fatty acids in green tea and dried green herbs*. Doctoral Thesis No. 14862,

492   ETH Zurich.

493   Sigrist, I. A., Giuseppe, G. G. M., & Amado, R. (2003). Aroma Compounds Formed from 3-Methyl-2,4-

494   nonanedione under Photooxidative Conditions. *Journal of Agricultural and Food Chemistry*, *51*,
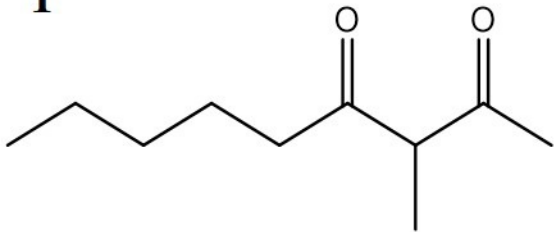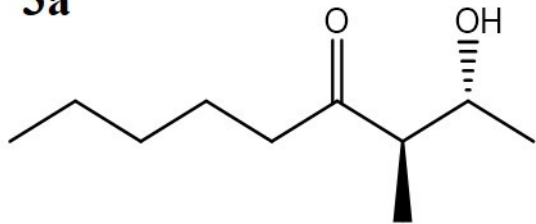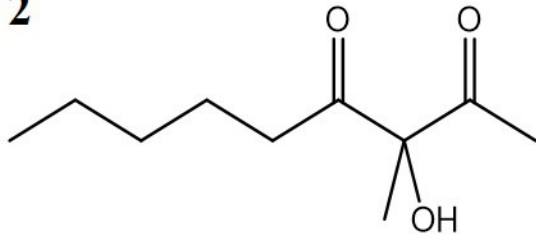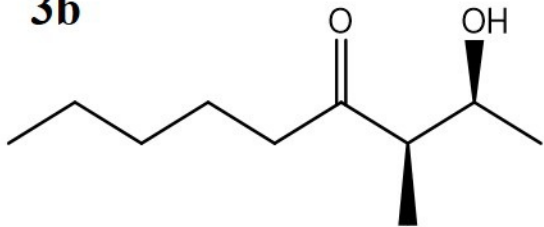
495   3426–3428.

496   Sigrist, I. A., Manzardo, G. G. G., & Amadò, R. (2002). Degradation Products in Dried Herbs and

497   Vegetables. *Food Technology*, *56*(6), 263–265.

498   Stephan, A., & Steinhart, H. (1999). Identification of Character Impact Odorants of Different Soybean

499   Lecithins. *Journal of Agricultural and Food Chemistry*, *47*, 2854–2859.

500   Triqui, R., & Bouchriti, N. (2003). Freshness Assessments of Moroccan Sardine (Sardina pilchardus):

501   Comparison of Overall Sensory Changes to Instrumentally Determined Volatiles. *Journal of*

502   *Agricultural and Food Chemistry*, *51*(26), 7540–7546.

503   van Den Dool, H., & Dec. Kratz, P. (1963). A generalization of the retention index system including

504   linear temperature programmed gas—liquid partition chromatography. *Journal of Chromatography*

505   *A*, *11*, 463–471.

506   Waterhouse, A. L., & Laurie, V. F. (2006). Oxidation of Wine Phenolics : A Critical Evaluation and

507   Hypotheses. *American Journal of Enology and Viticulture*, *3*, 306–313.

508   Yildiz, T., Canta, N., & Yusufoglu, A. (2014). Synthesis of new chiral keto alcohols by baker's yeast.
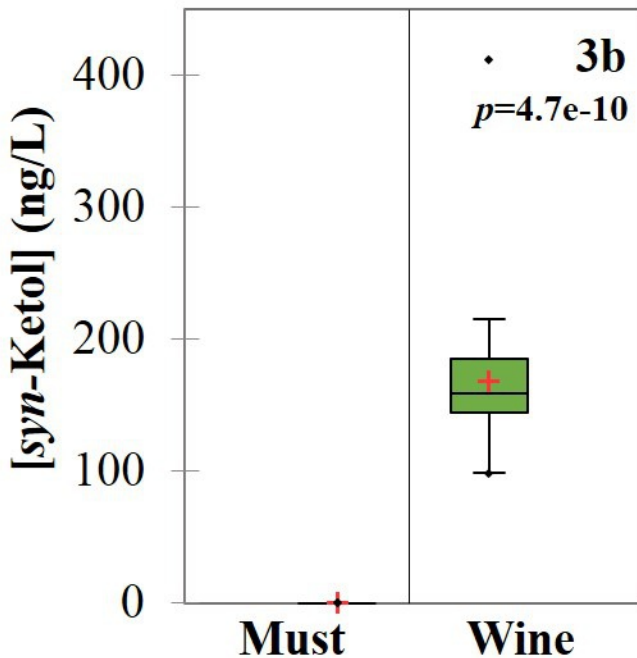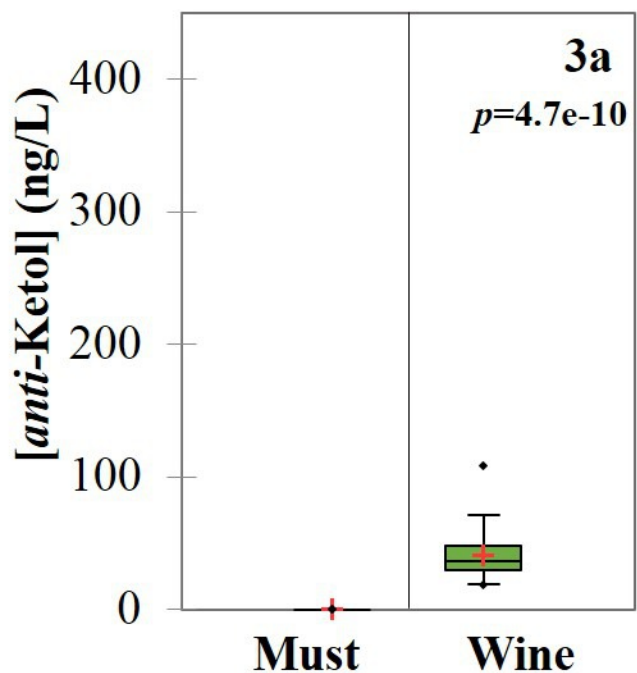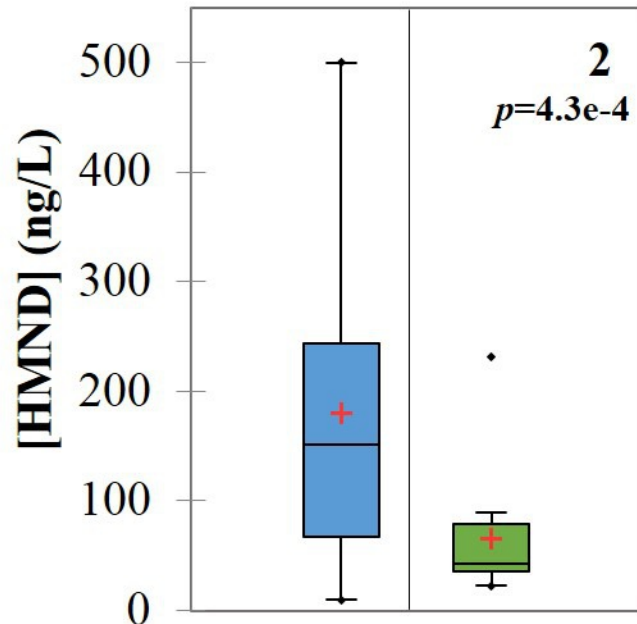
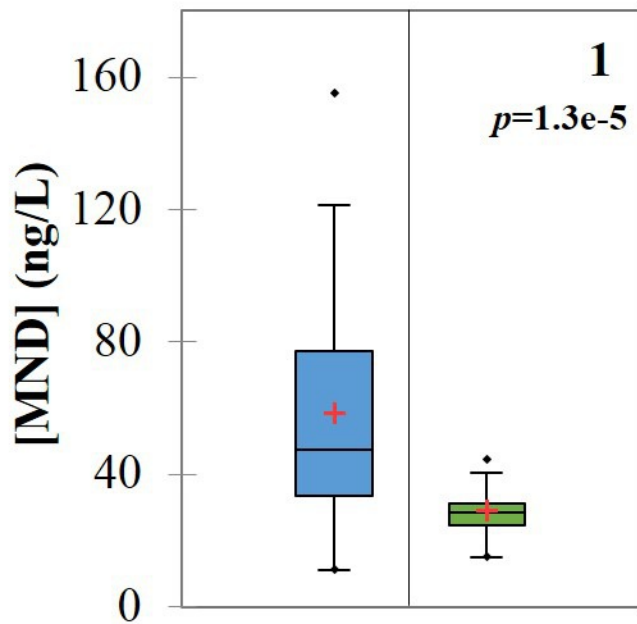509   *Tetrahedron: Asymmetry*, *25*, 340–347.

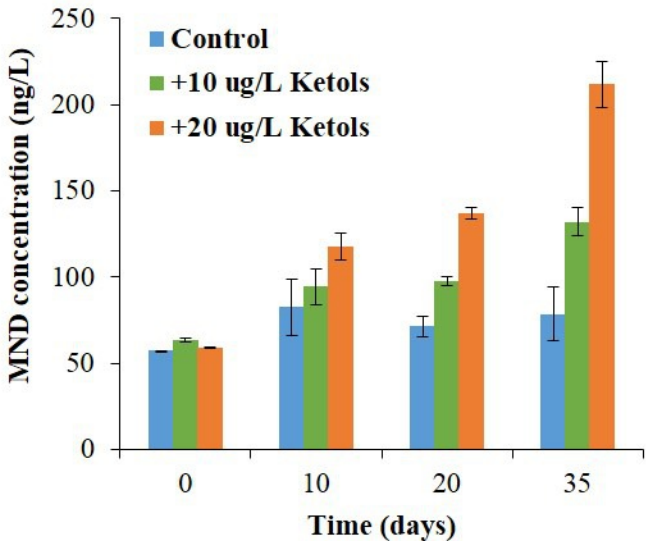510

511   **Figure Captions**

512   **Figure 1.** Molecular structures of compounds in this study: MND **1**, HMND **2**, *anti*-ketol **3a**, *syn*-ketol **3b**

513   **Figure 2.** Evolution of **(1)** MND, **(2)** HMND, **(3a)** *anti*-ketol, and **(3b)** *syn*-ketol through alcoholic

514   fermentation of musts (blue) to wine (green); n=32. **+** Concentration Mean ● Outliers

515   **Figure 3.** Evolution of MND in dry red wines supplemented with 10 and 20 µg/L ketols in the presence

516   of oxygen; n=3

1

2

3a

3b

Tables*: Identification and analysis of new α- and β-hydroxy ketones related to the formation of 3-methyl-

2,4-nonanedione in musts and red wines

Table 1. Method validation for the quantitation of MND **1**, HMND **2**, *anti*-ketol **3a** and *syn*-ketol **3b** in dry red wine and must

Compound	Linear Range ng/L	Linearity	R^2	RSD %	LOD ng/L	LOQ ng/L	Recovery %
Dry red wine							
1	24-285	y = 6.74E-03x – 6.35E-02	0.9925	3.2	7	24	96
2	13-215	y = 1.81E-04x – 6.15E-05	0.9949	9.1	4	13	97
3a	48-2370	y = 2.57E-04 – 2.48E-03	0.9957	8.2	15	48	99
3b	161-4110	y = 1.70E-04x – 1.22E-02	0.9967	6.4	48	161	93
Must							
1	11-294	y = 3.67E-03x – 5.04E-03	0.9916	6.9	3	11	93
2	54-300	y = 5.54E-05x + 1.06E-03	0.9922	10.3	16	54	94
3a	67-756	y = 1.12E-04x – 4.88E-04	0.9914	8.0	20	67	95
3b	92-370	y = 8.84E-05x + 7.24E-04	0.9989	7.5	28	92	94

Table 2. Summary of analyte concentrations in 167 wines, categorized by bottle aging time

Compound	Average Concentration (ng/L) (SD)[a]		p-value[d]
	Age < 6 years[b]	Age ≥ 6 years[c]	
MND **1**	50 (38)	118 (73)	5.92e-13**
HMND **2**	26 (16)	23 (16)	0.338
anti-ketol **3a**	282 (276)	411 (351)	1.04e-3*
syn-ketol **3b**	360 (195)	330 (136)	0.530
3a:3b	0.76 (0.37)	1.27 (0.66)	2.45e-7**

[a] Values in parentheses correspond to standard deviation of group. [b]n=64; [c]n=103; [d]p-values determined between the two groups of wines by Kruskal-Wallis test. *Significance with $p < 0.01$; **Significance with $p < 0.001$

Table 3. Contents of all analytes in dry red wines from various regions and vintage

Region[a]	Vintage	Grape Variety[b]	Concentration (ng/L)				Ratio 3a:3b
			MND **1**	HMND **2**	*anti*-ketol **3a**	*syn*-ketol **3b**	
Pomerol	2003	ME	203.2 ± 2.0	29.3 ± 1.9	313.2 ± 20.7	270.2 ± 19.8	1.16
FR	2013	ME	145.7 ± 11.7	18.1 ± 1.4	175.9 ± 2.1	262.5 ± 5.2	0.67
Pessac Leognan	2005	CS/ME	71.2 ± 2.4	nd[c]	163.9 ± 14.6	319.3 ± 21.0	0.51
FR	2015	CS/ME	96.5 ± 5.5	24.2 ± 1.7	102.9 ± 1.0	303.9 ± 15.8	0.34
Ticino	2006	ME	172 ± 10.8	40.5 ± 1.3	211.8 ± 35.7	248.0 ± 0.05	0.85
CH	2015	ME	73.4 ± 1.0	32.6 ± 7.2	114.1 ± 2.9	268.3 ± 38.3	0.43
Napa	2006	ME	406.6 ± 7.1	nd	1940.6 ± 48.8	811.2 ± 10.6	2.39
CA	2013	ME	147.8 ± 6.7	nd	292.4 ± 7.4	365.2 ± 23.3	0.80
Delaplane	2009	CS/ME	91.4 ± 12.4	16.6 ± 4.8	194.0 ± 12.8	537.2 ± 62.5	0.36
VA	2015	CS/ME	73.1 ± 7.0	46.1 ± 11.7	239.4 ± 35.5	673.5 ± 79.5	0.36

[a]Wines from each region came from the same chateau. [b]Tested wines were made from Merlot (ME) grapes or a blend of Cabernet Sauvignon and Merlot (CS/ME). [c]Not detected (nd)